Energy Efficiency Prediction Based on PCA-FRBF Model: A Case Study of Ethylene Industries

Zhiqiang Geng, Jie Chen, and Yongming Han

***Abstract*—Energy conservation and emission reduction in the ethylene industry is the main way to attain sustainable development, which can be achieved if the energy efficiency of petrochemical industries can be accurately analyzed and predicted. This paper proposes an improved radial basis function neural network based on fuzzy *C*-means (FCM) algorithm integrated with principal component analysis (PCA) technology (PCA-FRBF). The PCA is used to denoise and reduce dimensions of data to decrease the training time and errors of the modeling process. The FCM is used to separate every fuzzy class in input space and decide the number of neurons in hidden layer to overcome the shortcoming of setting them by experience subjectively. Meanwhile, the robustness and effectiveness of the PCA-FRBF model are validated through the standard data set from the University of California Irvine repository. Moreover, to predict the energy efficiency of ethylene plants, a multi-inputs and single-output model of energy efficiency is established based on the PCA-FRBF for monthly data of ethylene production process. We obtain a rational allocation of crude oil, fuel, steam, water, and electricity, and the greatest benefit of ethylene plants under different technologies. Finally, the empirical results show the effectiveness and practicability of the PCA-FRBF model applied to predict and guide the ethylene production in the petrochemical industry.**

***Index Terms*—Energy efficiency prediction, ethylene plants, fuzzy *C*-means (FCM) algorithm, principal component analysis (PCA), radial basis function (RBF), RBF neural network based on FCM algorithm (FRBF) integrated with PCA technology (PCA-FRBF).**

I. Introduction

THE petrochemical industry, especially the ethylene industry, plays an important role in assessing the industrialization of a country. In 2012, the average fuel plus power consumption (standard oil) was 628.6 kg for producing a ton of ethylene when China National Petroleum Corporation's ethylene production was 5110 kt/a [1]. The ethylene production capacity of China Petrochemical Corporation was 9475 kt/a, while producing a ton of ethylene needs the standard oil with the use of the fuel up to 579.59 kg [2]. Energy consumption costs accounted for over half of the operational costs of ethylene plants [3]. However, the average fuel plus power consumption (standard oil) was 440.2 kg for producing a ton of ethylene in the developed countries [4]. Obviously, the ethylene energy efficiency of the Chinese petrochemical industry is lower than that of the developed countries [4]. Thus, there is a big gap for improvement in the energy efficiency of the ethylene industry in China. Furthermore, studying the energy efficiency prediction of ethylene plants will achieve great economic benefits, and thus improve the environment and promote the sustainable development of the Chinese economy.

Currently, the mean method and optimal index method to analyze energy efficiency are commonly used by enterprises [5]. However, the two methods cannot introduce energy-saving knowledge into energy efficiency analysis and are not able to guide the actual state of energy efficiency analysis. Although the data fusion method has obtained better performance for energy efficiency analysis of ethylene plants, it did not take the impact factors of energy consumption indicators into account [6], [7]. Additionally, the method based on analytic hierarchy process (AHP) and data envelopment analysis (DEA) model has been widely applied to the efficiency evaluation of ethylene industries [8], [9], but crude oil was not taken into consideration. In allusion to the disadvantages of the existing energy efficiency analysis of the ethylene industry, this paper specifically proposes an improved radial basis function (RBF) neural network based on a fuzzy *C*-means (FCM) algorithm (FRBF) integrated with a principal component analysis (PCA) technology (PCA-FRBF).

Artificial neural network (ANN) has been used in several areas of chemical engineering applications, such as the modeling of a naphtha pyrolysis chemical process and predicting hydrocarbon density [10], [11]. Moreover, the ANN is widely applied in energy efficiency estimation and management, evaluation, and optimization fields [12]–[15].

The RBF neural network is one of the most popular networks among all ANNs. It was first designed by Broomhead and Lowe [16] in 1988. And the RBF is widely used in face recognition application [17], image processing [18], chaos time sequence prediction [19], and fault detection [20], etc. Recently, some researchers studied the RBF neural network on chemical engineering applications, including the prediction of the melt index on polypropylene polymerization products and the energy storage

Manuscript received May 5, 2015; revised August 17, 2015; accepted November 9, 2015. Date of publication February 19, 2016; date of current version July 17, 2017. This work was supported in part by the National Natural Science Foundation of China under Grant 61374166 and Grant 61533003, in part by the Fundamental Research Funds for the Central Universities under Grant YS1404 and Grant ZY1502, and in part by the Doctoral Fund of the Ministry of Education of China under Grant 20120010110010. This paper was recommended by Associate Editor E. Herrera-Viedma. *(Corresponding author: Yongming Han.)*

The authors are with the College of Information Science and Technology, Beijing University of Chemical Technology, and the Engineering Research Center of Intelligent PSE, Ministry of Education, Beijing 100029, China (e-mail: gengzhiqiang@mail.buct.edu.cn; 872814406@qq.com; hanym@mail.buct.edu.cn).

Color versions of one or more of the figures in this paper are available online at http://ieeexplore.ieee.org.

Digital Object Identifier 10.1109/TSMC.2016.2523936

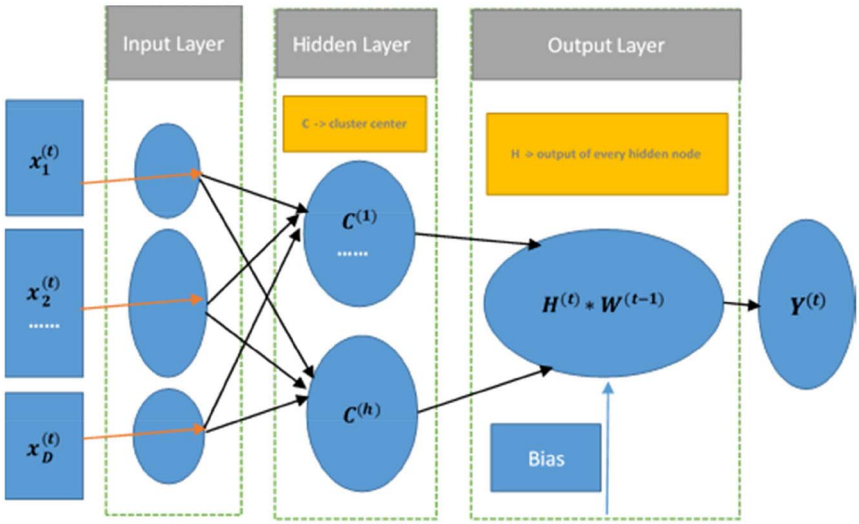

Fig. 1. RBF network structure diagram.

system [21], [22]. Although the RBF network has many advantages and been widely used, it has some shortcomings, such as the determination of the center of the hidden layer [23]. Therefore, Alam *et al.* [24] proposed an RBF network based on the FCM algorithm to obtain relative accurate modeling results. However, how to decide parameters of the clustering central and the fuzzy index in hidden nodes is not discussed.

The FCM algorithm is an extension of the K-means clustering algorithm by incorporating fuzziness into the original K-means clustering algorithm [25], and it is suitable for classifying a data set which has various types of inherent degradations. So it can solve the substantial shortcoming of the K-means algorithm. Meanwhile, the FCM is widely applied in the function approximation [26], fuzzy modeling of complex system [27], symbolic fuzzy classification [28], etc. Niros and Tsekouras [29] proposed a combined method of RBF and FCM, which made the RBF network faster and more efficient. Yuan *et al.* [30] studied a symmetry-based FCM algorithm to improve the effectiveness of RBF, and it is used in the prediction of fishery. However, many industrial data contain vast noise, while the clustering algorithms are always sensitive to outliers, so the original raw data should be denoised at first. According to PCA technology, several principal components (PCs) can represent the whole data set without losing significant features. In this way, the selected samples had less information redundancy and higher capacity of noise resistance [31]. In addition, the PCA technology could greatly reduce the dimensionality of the original data to a low-dimensional space, as it used all the original variables to generate the new PCs [32]–[34].

In this paper, to better analyze and predict the ethylene energy efficiency, we propose an integrated model of the PCA-FRBF. The noise existing in ethylene industrial data is eliminated, and the dimension of the original data set is reduced by using the PCA technology to improve the robustness of model and speed up the training time. The FCM algorithm is applied to realize a fuzzy clustering in the input space to decide the number of neurons in the hidden layer and overcome the shortcoming of setting hidden nodes randomly. Meanwhile, FCM is used to decrease the sensitivity of the data outlier. First standard data sets from the University of California Irvine (UCI) repository are used to validate the prediction capacity of the proposed model by comparing with the K-means RBF (KRBF) and FRBF model. Then, a predicted model using PCA-FRBF is established to analyze and predict the energy efficiency status of the ethylene procedure in the petrochemical industry.

The organization of this paper is as follows. Section I presents the research status of energy efficiency with the RBF, FCM, and PCA. The details of the FRBF-integrated PCA are described in Section II. The energy efficiency analysis and prediction framework based on the PCA-FRBF in ethylene industries are provided in Section III. Comparisons and parameters are discussed by standard data sets (Ionosphere data set [35], Zoo data set [36], and CMC data set [37]) in Section IV. Section V presents a case study about the energy efficiency prediction of ethylene industries based on the PCA-FRBF model. Finally, the discussion and the conclusion are given in Sections VI and VII, respectively.

II. RBF Neural Network Based on FCM

A. RBF Neural Networks

The RBF network has three layers: 1) an input layer; 2) a hidden layer; and 3) an output layer. The activation function in hidden layer is Gaussian function in general. The structure of the RBF is shown in Fig. 1.

The input layer has D units which connect the input space with the hidden layer. There is a clustering center $C^{(h)} = \{c_1^{(h)}, c_2^{(h)}, \ldots\ldots, c_D^{(h)}\}$ in every unit of hidden layer. The outputs of hidden layer are denoted as $H^{(t)} = \{h_{\text{out}_1}^{(t)}, h_{\text{out}_2}^{(t)}, \ldots\ldots, h_{\text{out}_h}^{(t)}\}$, and the weights between the hidden layer and output layer are trained by the gradient decent method based on the error propagation, which denotes

$$W^{(t)} = \begin{bmatrix} w_{11}^{(t)} & \cdots & w_{1n}^{(t)} \\ \vdots & \ddots & \vdots \\ w_{h1}^{(t)} & \cdots & w_{hn}^{(t)} \end{bmatrix}_{h*n}$$

where n denotes the unit of the output layer. Considering the tth input vector $X^{(t)} = \{x_1^{(t)}, x_2^{(t)}, \ldots\ldots, x_D^{(t)}\}$ and the hth cluster center $C^{(h)} = \{c_1^{(h)}, c_2^{(h)}, \ldots\ldots, c_D^{(h)}\}$, the Euclidean distance between $X^{(t)}$ and $C^{(h)}$ is obtained by the following equation:

$$\mathrm{Eu}_i^{(j)} = \sqrt{\sum_{q=1}^{D}\left(x_q^{(j)} - c_q^{(i)}\right)^2}. \tag{1}$$

The output of the hidden layer is given by the following equation:

$$h_{\mathrm{out}_k}^{(t)} = e^{-\frac{\left(\mathrm{Eu}_k^{(t)}\right)^2}{2\delta_k^2}} \tag{2}$$

where δ_k is the width of Gaussian function of the kth unit in hidden layer, which is fixed by the following equations:

$$\delta_k = \{\min < d_{k\to r} >, (k, r = 1, 2, \ldots\ldots, h) \cap (r \neq k)\} \tag{3}$$

$$d_{k\to r} = \left|\left|C^{(k)} - C^{(r)}\right|\right| = \sqrt{\sum_{j=1}^{D}\left(c_j^{(k)} - c_j^{(r)}\right)^2}. \tag{4}$$

The network output is shown in the following equation:

$$Y^{(t)} = \left\{H^{(t)} * W^{(t-1)}, t = 1, 2, \ldots\ldots, m, W^{(0)} \text{ is initial weight}\right\}. \tag{5}$$

The RBF network is established if the training meets a presetting error threshold. Otherwise, the weight is updated by the following equation:

$$W^{(t)} = \left\{W^{(t-1)} + \eta H^{(t)} * \left(\hat{Y}^{(t)} - Y^{(t)}\right), \eta(0, 1), \hat{Y}^{(t)} \text{ is theory output}\right\} \tag{6}$$

where $\hat{Y}^{(t)} = \{Y_1^{(t)}, Y_2^{(t)}, \ldots\ldots, Y_m^{(t)}\}$.

B. FRBF Model

In the real applications, most of the data belong to two or even more clusters. The FCM algorithm is more suitable for describing this situation. The traditional hard clustering method like K-means is sensitive to the initial centers, and the clustering results are fluctuated by different initial inputs. However, the FCM utilizes the fuzzy theory to find natural vague boundaries in data. It uses the membership degree to determine which cluster the data belong to. There are two key parameters in FCM algorithm: one is the clustering number c and the other is the fuzzy index p. Generally, c is far smaller than the number of clustering samples, and $p \in [1, +\infty)$, which usually takes a value between 1.5 and 2.5 [38]. The FCM will be much closer to the hard clustering method if p is undersize and will lose features of partition if p is oversize [39]. The FCM divide m samples with $X = \{X^{(1)}, X^{(2)}, \ldots\ldots, X^{(m)}\} \in R^D$ into h groups which are denoted as clustering centers $C = \{C^{(1)}, C^{(2)}, \ldots\ldots, C^{(h)}\} \in R^D$. D is the dimension of the vector $X^{(t)} = \{x_1^{(t)}, x_2^{(t)}, \ldots\ldots, x_D^{(t)}\}$ or $C^{(h)} = \{c_1^{(h)}, c_2^{(h)}, \ldots\ldots, c_D^{(h)}\}$, where $x_D^{(t)}$ is an attribute of the sample $X^{(t)}$. The membership degree matrix U is shown in the following equation:

$$U = \begin{bmatrix} u_1^{(1)} & \cdots & u_1^{(m)} \\ \vdots & \ddots & \vdots \\ u_h^{(1)} & \cdots & u_h^{(m)} \end{bmatrix}_{h*m} \tag{7}$$

where $u_h^{(m)}$ denotes the probability of the mth sample belonging to the hth clustering center, which takes a value between 0 and 1. The criterion function of the FCM is shown in the following equation:

$$\mathcal{H}(U; C) = \sum_{i=1}^{h}\mathcal{H}_i\left\{\sum_{i=1}^{h}\sum_{j=1}^{m}\left(u_i^{(j)}\right)^p\left(\mathrm{Eu}_i^{(j)}\right)^2 \middle| \sum_{i=1}^{h}u_i^{(j)} = 1, u_i^{(j)} \in [0, 1], h \in [2, m]\right\}. \tag{8}$$

The Euclidean distance is denoted by (1). Then, we minimize the criterion function $\mathcal{H}(U; C)$ and get the following equations:

$$C^{(i)} = \frac{\sum_{j=1}^{m}\left(u_i^{(j)}\right)^p X^{(j)}}{\sum_{j=1}^{m}\left(u_i^{(j)}\right)^p} \tag{9}$$

$$u_i^{(j)} = \frac{1}{\sum_{k=1}^{h}\left(\frac{Eu_i^{(j)}}{Eu_k^{(j)}}\right)^{2/(p-1)}}. \tag{10}$$

Finally, the FCM algorithm is described in Algorithm 1. Meanwhile, the FRBF model is established in Algorithm 2.

Algorithm 1 Obtain Clustering Centers

Input X, h, fuzzy index $p > 1$, T_{max}(*default* $T_{max} = 1000$), ε (*default* $\varepsilon = 0.001$)
Output U, C
Initialize U meets $\sum_{i=1}^{h} u_i^{(j)} = 1 \forall 1 \le j \le m$, $t = 1$, stop $= \varepsilon + 1$
While $t \le T_{max}$ && $stop > \varepsilon$
  $U_{expo} = U^p$, **For** $i = 1 \to h$
    $C^{(i)} = \sum_{j=1}^{m}\left(u_i^{(j)}\right)^p X^{(j)} \Big/ \sum_{j=1}^{m}\left(u_i^{(j)}\right)^p$
    Inner For $j = 1 \to m$
      $u_i^{(j)} = 1/\sum_{k=1}^{h}\left(\frac{Eu_i^{(j)}}{Eu_k^{(j)}}\right)^{2/(p-1)}$
    End Inner For
  End For
  $V^{(t)} = C$
  If $t > 1$
    $stop = \left|V^{(t)} - V^{(t-1)}\right|$
  End If
  $t + 1 \to t$
End While

Algorithm 2 Establish FRBF Model

Input X, $\hat{Y}$, h, T_{max}^{RBF} *(default* $T_{max}^{RBF} = 1000$*)*
ε_{max}^{RBF} *(default* $\varepsilon_{\max}^{\mathrm{RBF}} = 0.001$*),* η *(default*$\eta = 0.01$*)*
Output Y
Initialize $W^{(0)}$, $t^{RBF} = 1$, $stop^{RBF} = \varepsilon_{max}^{RBF} + 1$, C *(obtained by algorithm 1)*
$[m, D] = size(X)$, *m is samples and Disattributes of every sample*
$[m, n] = size\left(\hat{Y}\right)$, *m is samples and n is samples outputs*
For $k = 1 \rightarrow h$
$\delta_k = min\{d_{k\rightarrow r}\} for\ r = 1, 2, \ldots\ldots, h\ and\ k \neq r$
End For
For $t = 1 \rightarrow m$
$Eu_k^{(t)} = \sqrt{\sum_{q=1}^{D}\left(x_q^{(t)} - c_q^{(k)}\right)^2}, for\ k = 1, 2, \ldots\ldots, h$
$h_{out_k}^{(t)} = e^{-(Eu_k^{(t)})^2/2\delta_k^2},\ for\ k = 1, 2, \ldots\ldots, h$
$H^{(t)} = \left\{h_{out_k}^{(t)},\ for\ k = 1, 2, \ldots\ldots, h\right\}$
End For
While $t^{RBF} \leq T_{max}^{RBF}$
For $t = 1 \rightarrow m$
$Y^{(t)} = H^{(t)} * W^{(t-1)}$
$stop_t^{RBF} = 0.5 * \sum_{q=1}^{n}\left(\hat{Y}_q^{(t)} - Y_q^{(t)}\right)^2$
End For
$stop^{RBF} = \sqrt{\left(\sum_{t=1}^{m}\left(stop_t^{RBF}\right)^2\right)/m}$
If $stop^{RBF} \leq \varepsilon_{max}^{RBF}$
return
End If
$W^{(t^{RBF})} = W^{(t^{RBF}-1)} + \eta H^{(t^{RBF})} * \left(\hat{Y}^{(t^{RBF})} - Y^{(t^{RBF})}\right)$
$t^{RBF} + 1 \rightarrow t^{RBF}$
End While

III. FRBF Integrated PCA

A. PCA Technology

The PCA has been proved to be a vigoroso tool for denoising and reducing the dimension of the complex data. The relevance among all attributes is described by the convariance matrix, and the eigenvalue is obtained by the diagonalization of convariance matrix. Every eigenvalue in convariance matrix represents the energy of every attribute, and more energy expresses more information.

The PCA is a linear transformation from a set of variables to a new set of uncorrelated variables called PCs [40]. For reducing the dimensionality of multivariate data, PCs with the highest variances are retained while remaining PCs are discarded [41]. Eigenvectors of the covariance matrix can be obtained in turn using the singular value decomposition (SVD). The PCA process is described briefly as follows.

This matrix X is given in the following:

$$X = \begin{bmatrix} x_{11} & \cdots & x_{1p} \\ \vdots & \ddots & \vdots \\ x_{n1} & \cdots & x_{np} \end{bmatrix}_{n*p}$$

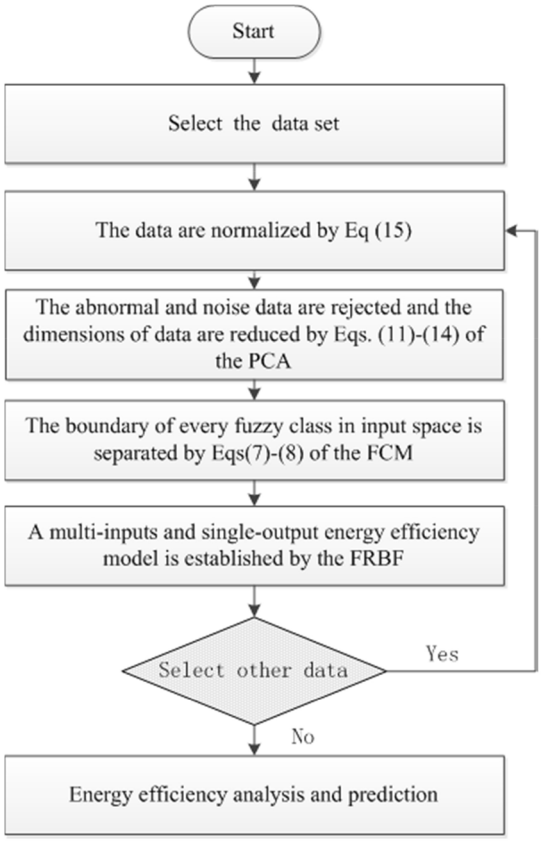

Fig. 2. Energy efficiency prediction procedure based on the PCA-FRBF.

which has n samples, and p attributes in each sample. First, normalize data matrix X by the following equations:

$$x_{ij}^{(\mathrm{norm})} = \left\{\frac{x_{ij} - \bar{x}_j}{\mathrm{SD}(x_j)},\quad i = 1, 2, \ldots\ldots, n \right. \\ \left. \text{and}\ \ j = 1, 2, \ldots\ldots, p\right\} \tag{11}$$

$$\bar{x}_j = \frac{1}{n}\sum_{i=1}^{n} x_{ij} \text{ and } \mathrm{SD}(x_j) \\ = \sqrt{\frac{1}{n-1}\sum_{i=1}^{n}\left(x_{ij} - \bar{x}_j\right)^2}, j = 1, 2, \ldots\ldots, p. \tag{12}$$

Then, calculate correlation coefficient matrix

$$R = \begin{bmatrix} r_{11} & \cdots & r_{1p} \\ \vdots & \ddots & \vdots \\ r_{p1} & \cdots & r_{pp} \end{bmatrix}_{p*p}$$

by the following equation:

$$r_{ij} = \left\{\frac{1}{n-1}\sum_{k=1}^{n} x_{ki}^{(\mathrm{norm})} * x_{kj}^{(\mathrm{norm})},\ i, j = 1, 2, \ldots\ldots, p\right\}. \tag{13}$$

Finally, according to the SVD algorithm, get the eigenvalue $F = (f_1, f_2, \ldots\ldots, f_p)$ of the correlation coefficient matrix and corresponding eigenvectors $\Psi = \begin{bmatrix} \psi_{11} & \cdots & \psi_{1p} \\ \vdots & \ddots & \vdots \\ \psi_{p1} & \cdots & \psi_{pp} \end{bmatrix}_{p*p}$.

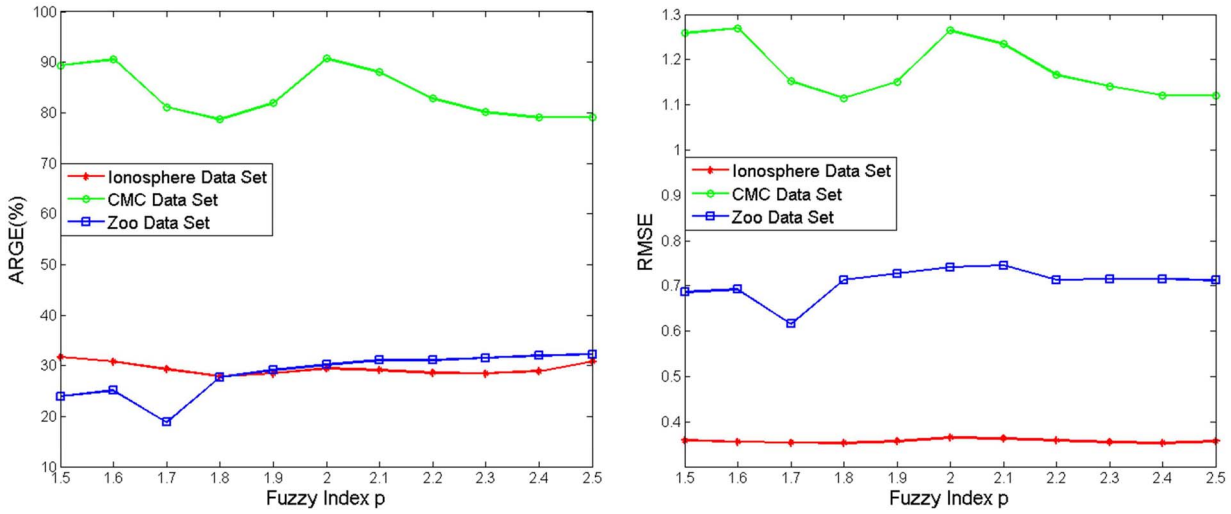

Fig. 3. Choice of fuzzy index for standard data sets.

The eigenvalue F expresses the variances of PCs. Generally, we only choose the first k largest PCs by the contribution rate (CR) calculated in the following equation:

$$\mathrm{CR}(\mathrm{PC}_i) = \frac{f_i}{\sum_{i=1}^{p} f_i} \tag{14}$$

where PC_i expresses the ith PC unit.

B. Data Preprocessing

Assume an original data set

$$X = (X^{(1)}, X^{(2)}, \ldots\ldots, X^{(m)})^T = (X_1, X_1, \ldots\ldots, X_D) = \begin{bmatrix} x_1^{(1)} & \cdots & x_D^{(1)} \\ \vdots & \ddots & \vdots \\ x_1^{(m)} & \cdots & x_D^{(m)} \end{bmatrix}.$$

Because the dimension of each attribute is different in general, the data set X is normalized by the following equation:

$$\bar{x}_j^{(t)} = \begin{cases} \dfrac{x_j^{(t)} - X_j^{\min}}{X_j^{\max} - X_j^{\min}}, & \text{if } x_j^{\max} \neq x_j^{\min} \\ -1, & \text{other} \end{cases} \tag{15}$$

where $X_j^{\max} = \max\{x_j^{(1)}, x_j^{(2)}, \ldots\ldots, x_j^{(m)}\}$, $X_j^{\min} = \min\{x_j^{(1)}, x_j^{(2)}, \ldots\ldots, x_j^{(m)}\}$. Correspondingly, the inverse-normalized procedure is obtained by the following equation:

$$x_j^{(t)} = \bar{x}_j^{(t)} * \left(X_j^{\max} - X_j^{\min}\right) + X_j^{\min}. \tag{16}$$

C. PCA-FRBF Model

Based on above analysis, we propose a more powerful method with seamless integration of the PCA and FRBF model. PCA gets rid of the noise and reduces the dimension of data set attributes, which are taken as the input variables of the FRBF model. Then, the FRBF network model is established to analyze and predict the energy efficiency. The overall procedure of energy efficiency prediction using the proposed PCA-FRBF is shown in Fig. 2.

TABLE I
SPECIFICATION OF STANDARD DATA SETS

Data Sets	*#Samples*		*#Attributes*	
	Training	Testing	Inputs	Output
Ionosphere	224	127	34	1
Zoo	68	33	16	1
CMC	1000	473	9	1

IV. Parameter Determination and Algorithm Comparison Based on Standard Data Sets

In order to validate the effectiveness and robustness of the PCA-FRBF model, we use some standard data sets from the UCI repository, the specification of which is listed in Table I.

We build the KRBF, the FRBF, and the PCA-FRBF network model by setting a learning factor as 0.01, the training times as 1000, and the maximum allowed error as 0.001 in the error back-propagation procedure. The average relative generalization error (ARGE) and root mean square error (RMSE) are obtained by the following equations:

$$\begin{cases} \begin{cases} \mathrm{RGE}_i = \mathrm{Abs}\left(\dfrac{\mathrm{NetOut}_i^{\mathrm{inver}} - \mathrm{ExpectOut}_i^{\mathrm{inver}}}{\mathrm{ExpectOut}_i^{\mathrm{inver}}}\right), \\ \qquad \text{if } \mathrm{ExpectOut}_i^{\mathrm{inver}} \neq 0 \\ \mathrm{RGE}_i = \mathrm{Abs}\left(\mathrm{NetOut}_i^{\mathrm{inver}} - \mathrm{ExpectOut}_i^{\mathrm{inver}}\right), \ \text{else} \end{cases} \\ \mathrm{ARGE} = \dfrac{\sum_{i=1}^{n} \mathrm{RE}_i}{n} * 100 \end{cases} \tag{17}$$

$$\begin{cases} \mathrm{MSE}_i = \left(\mathrm{NetOut}_i^{\mathrm{norm}} - \mathrm{ExpectOut}_i^{\mathrm{norm}}\right)^2 \\ \mathrm{RMSE} = \sqrt{\dfrac{\sum_{i=1}^{n} \mathrm{MSE}_i}{n}} \end{cases} \tag{18}$$

where $\mathrm{NetOut}_i^{\mathrm{inver}}$ is the inverse normalized network output for all samples, $\mathrm{ExpectOut}_i^{\mathrm{inver}}$ is the expected output, and $\mathrm{NetOut}_i^{\mathrm{norm}}$ is the normalized network output for all samples, $i = 1, 2, \ldots\ldots, n$.

In order to choose a suitable fuzzy index, we perform the experiments repeatedly by changing the fuzzy index from 1.5 to 2.5 with interval of each step 0.1 for standard data sets. And we obtain the curves that the ARGE and RMSE vary with different fuzzy indexes are shown in Fig. 3. It can be seen

TABLE II
COMPARISON OF THE ARGE AND RMSE OF KRBF, AND FRBF AND PCA-FRBF

Data Sets	Nodes	KRBF		FRBF		PCA-FRBF		
		ARGE	RMSE	ARGE	RMSE	ARGE	RMSE	PCs
Ionosphere	3	0.33	0.37	0.32	0.36	0.35	0.37	20
	5	0.29	0.38	0.28	0.35	0.27	0.34	
	6	0.28	0.37	0.28	0.35	0.27	0.35	
	7	0.28	0.35	0.28	0.35	0.27	0.35	
Zoo	3	0.52	1.66	0.40	1.70	0.35	1.74	7
	5	0.27	0.73	0.20	0.63	0.18	0.61	
	6	0.27	0.75	0.38	0.90	0.27	0.70	
	7	0.25	0.70	0.39	0.92	0.25	0.70	
CMC	10	0.94	1.32	0.89	1.25	0.89	1.25	7
	15	0.90	1.27	0.81	1.13	0.78	1.10	
	28	0.86	1.22	0.78	1.09	0.76	1.09	

from Fig. 3 that the ARGE and RMSE of the data set are the smallest when the fuzzy index p is in the range 1.6–1.9 compared with those whose fuzzy indexes are not in that range. Therefore, the fuzzy index p is set as 1.8 for standard data sets.

Because the principle of PCA is to ensure that the accumulated variance contribution rate (AVCR) is no less than 0.9 [42], so we obtain 20 PCs of Ionosphere data set, seven PCs of Zoo data set, and seven PCs of CMC data set when the AVCR is up to 0.9. Meanwhile, we increase the nodes of FRBF network and perform the experiment again. The ARGE and the RMSE are listed in Table II.

It can be seen from Table II that both ARGE and RMSE of the PCA-FRBF model are the best when the hidden nodes are set as 5 for Ionosphere and Zoo data sets and set as 15 for CMC data set. The ARGE and the RMSE of FRBF are close to that of PCA-FRBF when nodes of hidden layer increase; however, the computing time is longer along with the increasing of hidden nodes. Therefore, we set the hidden nodes of PCA-FRBF model as 5 for Ionosphere and Zoo data sets and set the hidden nodes of PCA-FRBF model as 15 for CMC data set. According to Table II, the effectiveness of the PCA-FRBF model is validated.

TABLE III
FEATURES OF DIFFERENT METHODS INTRODUCED IN THIS PAPER

Method	Characteristics
Simple Sum	① Simple and convenient ② Subjectivity is too strong, not considering data weights among different ethylene plants
AHP	① More objective and weights distribute better ② Not considering the effect of crude oil on the energy consumption such as water , electricity, steam and fuel
DEA	① Objective, consider the effect of crude oil on the ethylene production energy consumption, water , electricity, steam and fuel ② Multi-input and multi- output and decision-making units have restrictions
KRBF	① Objective, and The K-Means can decide the number of neurons in hidden layer. ② Unstable, The K-Means is sensitive to noise, and the modeling accuracy is poor.
FRBF	① Objective, and The FCM can decide the number of neurons in hidden layer. ② Stable, the modeling accuracy is better, however, it is sensitive to outlier.
PCA-FRBF	① Objective, The FCM can decide the number of neurons in hidden layer. ② The PCA can denoise and reduce dimensions of data sources. Robustness is good, and modeling accuracy is better.

V. CASE STUDY: ENERGY EFFICIENCY PREDICTION OF THE ETHYLENE PRODUCTION INDUSTRY

In order to make the model a better application in the real world, we choose the ethylene production monthly data from 2009 to 2013 [43], [44]. In the ethylene production system, different ethylene production plants may be quite different in division of energy utilization boundary. In order to make a unanimous criterion of computing energy efficiency objectively, the main energy consumption as follows: the crude oils including naphtha, light diesel oil, raffinate, hydrogenation tail oil#1, hydrogenation tail oil#2, carbon345 (the sum of carbon3, carbon4, and carbon5), and other force; the electricity; steams including super-high pressure steam, high pressure steam, middle, and low-pressure steam; the water including recycle water, boiler water, industrial water, and other water; fuel including light oil, fuel gas, and heavy oil; and $N2$ and compressing air. Because of the lowest consumption of $N2$ and compressing air among energy types, they were not computed considering energy efficiencies of ethylene product system. And based on energy consumption calculation method of petroleum chemical design (SH/T3110-2001) [45], the measure unit of energy consumption parameters of steams, electricity, water, and fuel are translated into the uniform GJ of per ton of ethylene. Meanwhile, the ethylene, propylene, and C_4 are the main productions of the ethylene plants, whose unit is ton. Therefore, the consumption of crude oils, fuel, water, steams, and electricity are taken as the inputs of ethylene systems, and the production sum of propylene, ethylene, and C_4 are taken as the outputs [8], [9], [43], [44].

The energy efficiency data are added up directly, without considering the distribution of each weight. AHP hierarchical model fuses the energy efficiency data under every technology, without considering the effect of the major crude oil [8]. The efficiency discrimination of the DEA model is poor [9]. Compared with the RBF and the FRBF from the ethylene data, the objectivity and the robustness of the PCA-FRBF model have been proved.

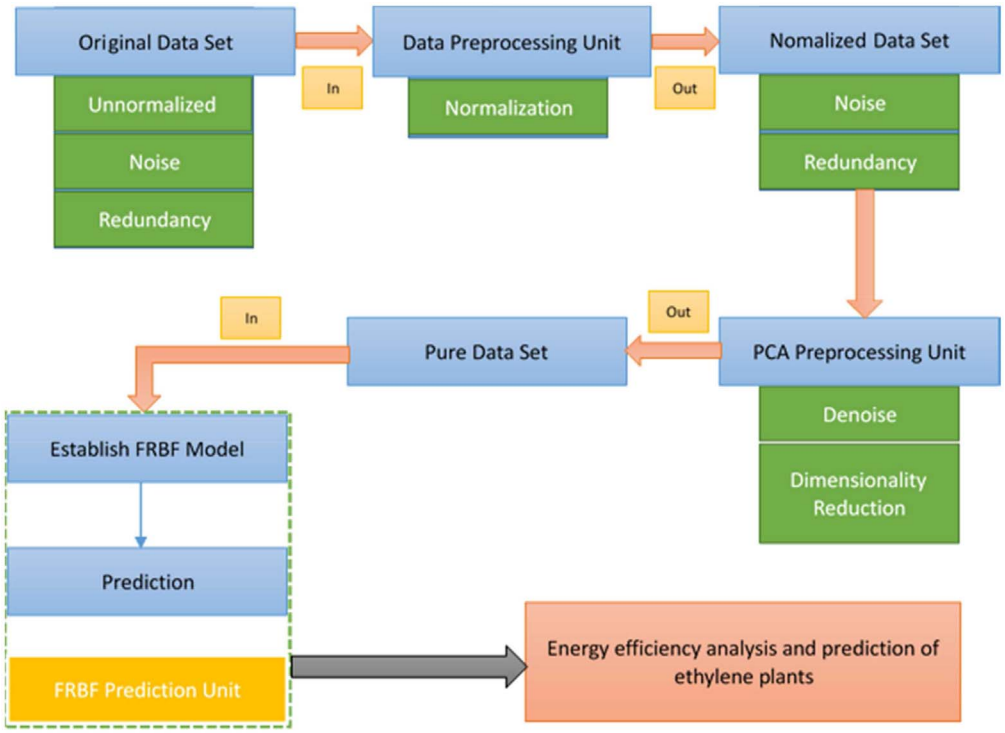

Fig. 4. Energy efficiency prediction model of the ethylene plants.

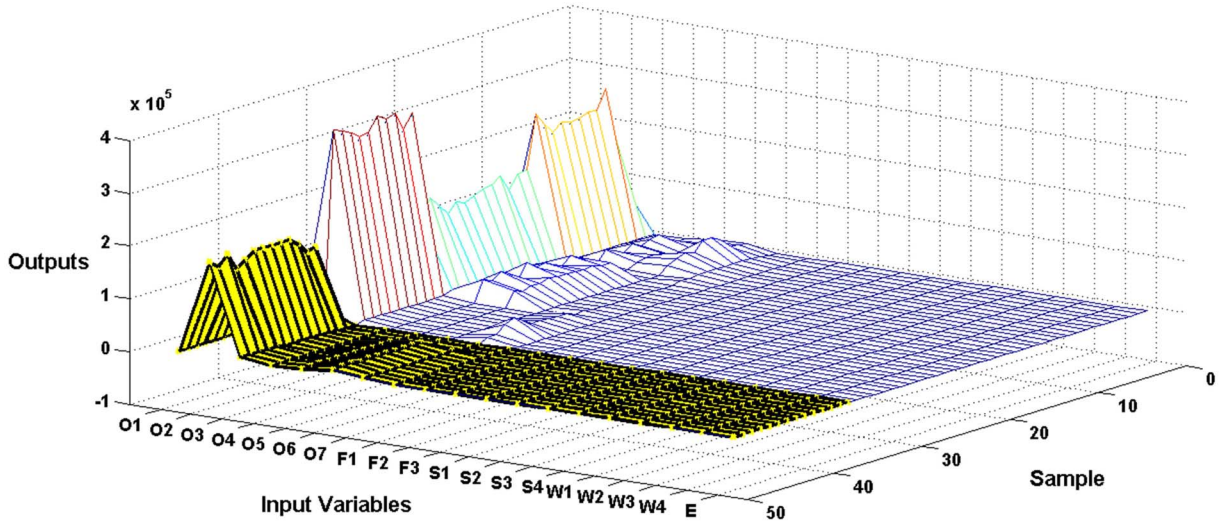

Fig. 5. Two class plants' inputs with different productive technology.

Table III shows the features of different methods introduced in this paper.

The energy efficient analysis and prediction of ethylene industries are processed by using the PCA-FRBF model in Fig. 4.

In order to analyze the relationships of ethylene plants under different technologies, it is essential to use the separation technology and the S&W technology with the scale of 800 000 ton ethylene per year in the empirical analysis. There are six ethylene plants of the separation technology in China, and they are Qilu ethylene, Saike ethylene, Maoming ethylene, Yangtze ethylene, Yanshan ethylene, and Tianjin ethylene. And there are two ethylene plants of the S&W technology: 1) Yangba ethylene and 2) Shanghai ethylene.

All of the required fuels, steams, water, and electricity of partial ethylene plants in 2010 are described at Fig. 5. And the corresponding data are shown in Table IV. In Fig. 5, these areas with yellow color express the inputs of S&W technology in 2010, and other areas indicate the inputs of the separation technology in 2010.

First, we choose three models: 1) KRBF; 2) FRBF; and 3) PCA-FRBF, and they are used to illustrate the efficiency of the proposed model. Meanwhile, we build these models using the ethylene production monthly data of 2011, and

TABLE IV
REAL DATA OF TWO CLASS PLANTS' INPUTS WITH DIFFERENT PRODUCTION TECHNOLOGIES

Inputs	S&W technology		Separation technology					
	Plan1	Plan2	Plan3	Plan4	Plan5	Plan6	Plan7	Plan8
O1	0	26500	0	0	0	0	0	0
O2	85480	23585	160691	173768	161954	150186	182434	164061
O3	0	0	2592	3383	5784	4813	6044	5605
O4	1863	0	0	0	0	0	0	0
O5	8486	0	2363	2671	2993	3426	3731	3057
O6	9905	159	10199	11164	11585	9195	13094	11717
O7	0	0	3495	3625	3718	3010	3668	4053
F1	0.49	0.5	0.5	0.49	0.48	0.51	0.49	0.48
F2	0	0	0	0	0	0	0	0
F3	0	0	0	0	0	0	0	0
S1	1.89	3.13	-0.02	-0.01	-0.01	-0.01	-0.01	-0.01
S2	-0.09	-2.18	0.92	1.25	1.07	1.48	0.9	1.17
S3	-0.94	-0.11	-0.59	-0.87	-0.33	-0.41	-0.37	-0.72
S4	-1.3	-0.09	-0.11	-0.08	-0.02	-0.07	-0.04	-0.03
W1	786.43	450	491.79	492.15	571.47	631.76	507.21	544.22
W2	1.29	0.26	0.15	0.46	0.16	0.13	0.6	0.25
W3	4.18	4.11	1.76	1.76	1.96	1.87	1.65	1.59
W4	0	0	0.2	0.29	0.14	0.15	0.14	0.12
E	1.01	0.91	2	1.93	2.11	2.2	2.01	2.19

Note: O1~O7 are oil (Unit: Ton); F1~F3 are fuel (Unit: GJ/Tons of ethylene); S1~S4 are steam(Unit: GJ/Tons of ethylene); W1~W4 are water (Unit: GJ/Tons of ethylene); E is electric (Unit: GJ/Tons of ethylene).

TABLE V
FEATURES OF THE ETHYLENE PRODUCTION DATA

Data	Samples	# Attributes	
		Inputs	Output
Train (In 2011)	210	19	1
Test (In 2012)	301	19	1

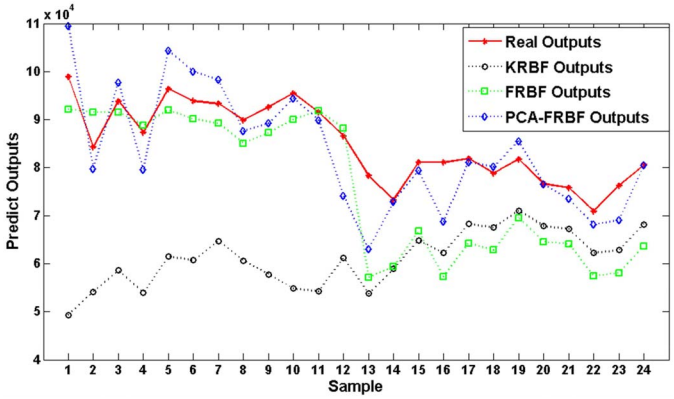

Fig. 6. Predicted results of KRBF, FRBF, and PCA-FRBF model.

predicting the outputs of ethylene plants of 2012. And the features of the data set are shown in Table V.

According to the PCA experiments, we get ten PCs when the AVCR is up to 90%. Then in this experiment, we set the hidden nodes as 5 according to the standard testing, the learning factor as 0.01, the training time as 1000, and the maximum allowed error as 0.001. And we perform the experiments choosing the fuzzy index as 1.59 for ethylene industrial data as the same as the choice of fuzzy index for standard data sets. Finally, the results with partial data are predicted in Fig. 6.

In Fig. 6, the ARGE of the KRBF and the FRBF and the PCA-FRBF is 11.8175%, 12.3341%, and 5.5529%, respectively. The PCA-FRBF model is more precise than the KRBF model and the FRBF model. Meanwhile, sample#1 to sample#12 show that the predictions of the KRBF model stay away from the real outputs, and sample#14 to sample#24 show that the predicted results of the FRBF model stay away from the real outputs. These show that the PCA-FRBF model is more stable than the KRBF model and the FRBF model. Therefore, we utilize the PCA-FRBF model to predict the ethylene efficiency.

We establish the PCA-FRBF model using the partial ethylene production data in 2009, which has 210 samples. And the parameters set as: the hidden node is 6, the fuzzy index is 1.8, the learning factor is 0.01, and the training time is 1000. According to the PCA technology, we get the eigenvalues and the AVCR of every PC, which described in Table VI. Meanwhile, we describe the AVCR of every PC, which is presented in Fig. 7. Therefore, we will choose the first eight PCs when the AVCR is more than 0.9. Then, we predict the sum of outputs of the S&W technology and the separation technology in 2010. The results are shown in Fig. 8. And the statistics of Fig. 8 are shown in Table VII.

It can be seen from Fig. 8 that the generalization ability of the PCA-FRBF model is strong, and its ARGE is 4.1196%. Therefore, we can take the results predicted by the PCA-FRBF model as the approximate real outputs. Furthermore, we can see that the production will increase even though the input variable decrease from Tables IV and VII. Such as the Plant1 of the S&W technology needs 8486 ton crude oil, 0.49 GJ/tons of ethylene fuel, and 786.43 GJ/tons of ethylene water, and the output is about 53 901.49 tons. Nevertheless, the output will increase approximately 33 790.22 tons when reducing 5493 tons crude oil, 0.01 GJ/tons of ethylene fuel, and 214.96 GJ/tons of ethylene water. And for Plant7 of the separation technology, the output will increase approximately 46 030.32 tons when reducing 4755 tons feed oil and 279.22 GJ/tons of ethylene water. From above analysis and prediction, we know how to increase the energy efficiency of

TABLE VII
PREDICTIONS OF PLAN1, PLAN5, PLAN6, PLAN7, AND PLAN8 OF TABLE IV

Technology	S&W technology	Separation technology			
	Plan1	Plan5	Plan6	Plan7	Plan8
Prediction	53901.49	87691.71	71655.21	99931.81	84854.87

TABLE VI
EIGENVALUES AND AVCR OF EVERY PC

PCs (*ordered*)	Eigenvalues	AVCR
1-th	0.5394	0.2826
2-th	0.3276	0.4543
3-th	0.2607	0.5909
4-th	0.1746	0.6824
5-th	0.1421	0.7568
6-th	0.1035	0.8111
7-th	0.0921	0.8593
8-th	0.0843	0.9035
9-th	0.0472	0.9282
10-th	0.0356	0.9469
11-th	0.0297	0.9624
12-th	0.0253	0.9757
13-th	0.0204	0.9864
14-th	0.0125	0.9929
15-th	0.0066	0.9963
16-th	0.0036	0.9982
17-th	0.0019	0.9992
18-th	0.0012	0.9998
19-th	0.0003	1.0000

Note: the data sources predicted are derived from the Plan1, Plan5, Plan6, Plan7 and Plan8 of TABLE IV.

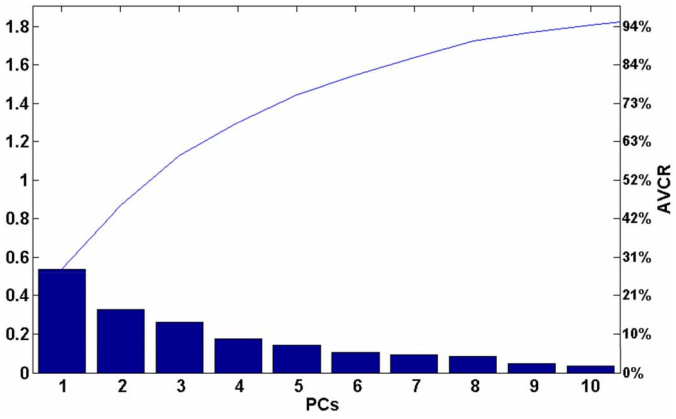

Fig. 7. AVCR of the first ten PCs.

the ethylene plants with the different technologies. Meanwhile, the energy efficiency of ethylene plants of the separation technology is superior to that of the S&W technology under the same production scale. In order to obtain supreme benefit, this proposed method can guide us how to allocate the raw material according to the production technology.

VI. DISCUSSION

First, we start energy efficiency analysis by predicting outputs of ethylene production plants under the same scale and different technologies based on the production data. As can be seen from experimental results, we can obtain rational allocation of crude oil, fuel, steam, water, and electricity, and

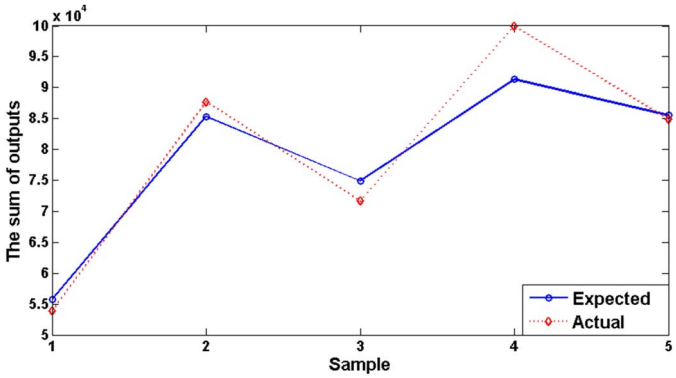

Fig. 8. Predicted results of the S&W technology and the separation technology.

the optimal production situation under the different technologies, and even if we reduce some inputs of raw material, the production of the ethylene will still increase. Therefore, the PCA-FRBF model can guide us to analyze and predict the energy efficiency of ethylene plants.

Second, the robustness and effectiveness of PCA-FRBF model are validated through the standard data sources from the UCI repository. Meanwhile, compared with the RBF and the FRBF from the standard testing and the ethylene production data, the objectivity and robustness of PCA-FRBF model have been proved. However, how to obtain the clustering number and fuzzy index automatically according to different data sets is our further work.

Third, the model is applied to predict the energy efficiency of ethylene plants effectively, and the parameters of model are adjusted by experiments. Therefore, we will improve our model by adjusting parameters automatically, such as designing a self-organizing PCA-FRBF model, which is more suitable to the real-world applications.

VII. CONCLUSION

In this paper, we propose a PCA-FRBF model, which can make ethylene energy analysis better. First, the dimensions of source data are greatly reduced using the PCA technology. Second, the boundary of every fuzzy class in input space is separated by the FCM. Meanwhile, from the prediction of ethylene plants with the same scale and different technologies, we can obtain the greatest benefits of ethylene plants under different technologies by the proposed PCA-FRBF model. Furthermore, the ethylene energy efficiency can be improved effectively according to the information on energy consumption factors provided by the study. Moreover, it is also suitable to serve as a guide for obtaining rational allocation of ethylene production resources based on the information.

In our further studies, we will separate output indicators (including human factors and economies) into desirable (good)

outputs and undesirable (bad) outputs for the energy efficiency prediction of the ethylene plants in the petrochemical industry. Moreover, we will investigate and integrate other methods, such as Malmquist production efficiency and ANN, to predict the energy efficiency under different scales, input-output energy measuring of ethylene plants, and to compare with the current work. Furthermore, the PCA-FRBF model could be applied to the energy efficiency analysis of other process plants.

REFERENCES

[1] L. J. Zhang and J. Liu, "Review of Petrochina's ethylene production in 2012," *Ethylene Ind.*, vol. 25, no. 1, pp. 7–10, 2013.

[2] W. Y. Ji, Y. H. Xu, and X. Guo, "Review of Sinopec's ethylene production in 2012," *Ethylene Ind.*, vol. 25, no. 1, pp. 1–6, 2013.

[3] T. Ren, M. Patel, and K. Blok, "Olefins from conventional and heavy feedstocks: Energy use in steam cracking and alternative processes," *Energy*, vol. 31, no. 4, pp. 425–451, 2006.

[4] Department of Energy Statistics, *National Bureau of Statistics, People's Republic of China, China Energy Statistical Yearbook 2013*. Beijing, China: China Stat. Press, 2013.

[5] J. A. Baileya, R. Gordona, D. Burtonb, and E. K. Yiridoe, "Energy conservation on Nova Scotia farms: Baseline energy data," *Energy*, vol. 33, no. 7, pp. 1144–1154, 2008.

[6] Z. Q. Geng, Y. M. Han, Y. Y. Zhang, and X. Y. Shi, *Data Fusion-Based Extraction Method of Energy Consumption Index for the Ethylene Industry* (LNCS 6329). Heidelberg, Germany: Springer, 2010, pp. 84–92.

[7] Z. Q. Geng, X. Y. Shi, X. B. Gu, and Q. X. Zhu, "Hierarchical linear optimal fusion algorithm and its application in ethylene energy consumption indices acquisition," *J. Chem. Ind. Eng. China*, vol. 61, no. 8, pp. 2056–2060, 2010.

[8] Z. Q. Geng, X. B. Gu, and Q. X. Zhu, "Study on dependent function analytic hierarchy process model for energy efficiency virtual benchmark and its applications in ethylene equipments," *J. Chem. Ind. Eng. China*, vol. 62, no. 8, pp. 2372–2377, 2011.

[9] Z.-Q. Geng, Y. M. Han, and C.-P. Yu, "Energy efficiency evaluation of ethylene product system based on density clustering data envelopment analysis model," *Adv. Sci. Lett.*, vol. 9, no. 1, pp. 735–741, 2012.

[10] E. Egon, Z. Bělohlav, T. Vaněk, P. Zámostný, and T. Herink, "ANN modelling of pyrolysis utilising the characterisation of atmospheric gas oil based on incomplete data," *Chem. Eng. Sci.*, vol. 62, nos. 18–20, pp. 5021–5025, 2007.

[11] R. Haghbakhsh, H. Adib, P. Keshavarz, M. Koolivand, and S. Keshtkari, "Development of an artificial neural network model for the prediction of hydrocarbon density at high-pressure, high-temperature conditions," *Thermochim. Acta*, vol. 551, pp. 124–130, Jan. 2013.

[12] G. Jahedi and M. M. Ardehali, "Wavelet based artificial neural network applied for energy efficiency enhancement of decoupled HVAC system," *Energy Convers. Manag.*, vol. 54, no. 1, pp. 47–56, 2012.

[13] H. Taghavifar and A. Mardani, "Applying a supervised ANN (artificial neural network) approach to the prognostication of driven wheel energy efficiency indices," *Energy*, vol. 68, pp. 651–657, Apr. 2014.

[14] T. Teich, F. Roessler, D. Krainc, and S. Franke, "Design of a prototype neural network for smart homes and energy efficiency," *Proc. Eng.*, vol. 69, no. 1, pp. 603–608, 2014.

[15] I. Monedero *et al.*, "Decision system based on neural networks to optimize the energy efficiency of a petrochemical plant," *Expert Syst. Appl.*, vol. 39, no. 10, pp. 9860–9867, 2012.

[16] D. S. Broomhead and D. Lowe, "Multivariable functional interpolation and adaptive networks," *Complex Syst.*, vol. 2, no. 3, pp. 321–355, 1988.

[17] J. Haddadnia, K. Faez, and M. Ahmadi, "A fuzzy hybrid learning algorithm for radial basis function neural network with application in human face recognition," *Pattern Recognit.*, vol. 36, no. 5, pp. 1187–1202, 2003.

[18] J. Alam, M. Hassan, A. Khan, and A. Chaudhry, "Robust fuzzy RBF network based image segmentation and intelligent decision making system for carotid artery ultrasound images," *Neurocomputing*, vol. 151, pp. 745–755, Mar. 2015.

[19] Y.-K. Yang *et al.*, "A novel self-constructing radial basis function neural-fuzzy system," *Appl. Soft Comput.*, vol. 13, no. 5, pp. 2390–2404, 2013.

[20] M. M. Kamal, D. W. Yu, and D. L. Yu, "Fault detection and isolation for PEM fuel cell stack with independent RBF model," *Eng. Appl. Artif. Intell.*, vol. 28, pp. 52–63, Feb. 2014.

[21] Z. Y. Zhang, T. Wang, and X. G. Liu, "Melt index prediction by aggregated RBF neural networks trained with chaotic theory," *Neurocomputing*, vol. 131, pp. 368–376, May 2014.

[22] W.-Y. Chang, "Estimation of the state of charge for a LFP battery using a hybrid method that combines a RBF neural network, an OLS algorithm and AGA," *Int. J. Elect. Power Energy Syst.*, vol. 53, pp. 603–611, Dec. 2013.

[23] M. Gan, H. Peng, and X.-P. Dong, "A hybrid algorithm to optimize RBF network architecture and parameters for nonlinear time series prediction," *Appl. Math. Model.*, vol. 36, no. 7, pp. 2911–2919, 2012.

[24] J. Alam, M. Hassan, A. Khan, and A. Chaudhry, "Robust fuzzy RBF network based image segmentation and intelligent decision making system for carotid artery ultrasound images," *Neurocomputing*, vol. 151, pp. 745–755, Mar. 2015.

[25] D. L. Pham, "Spatial models for fuzzy clustering," *Comput. Vis. Image Understand.*, vol. 84, no. 2, pp. 285–297, 2001.

[26] A. Guillén *et al.*, "Using fuzzy logic to improve a clustering technique for function approximation," *Neurocomputing*, vol. 70, nos. 16–18, pp. 2853–2860, 2007.

[27] S.-K. Oh, W.-D. Kim, W. Pedrycz, and K. Seo, "Fuzzy radial basis function neural networks with information granulation and its parallel genetic optimization," *Fuzzy Sets Syst.*, vol. 237, pp. 96–117, Feb. 2014.

[28] K. Mali and S. Mitra, "Symbolic classification, clustering and fuzzy radial basis function network," *Fuzzy Sets Syst.*, vol. 152, no. 3, pp. 553–564, 2005.

[29] A. D. Niros and G. E. Tsekouras, "A novel training algorithm for RBF neural network using a hybrid fuzzy clustering approach," *Fuzzy Sets Syst.*, vol. 193, pp. 62–84, Apr. 2012.

[30] H. C. Yuan, X. Q. Shen, and X. J. Chen, "Prediction of fishing ground based on RBF neural network," *Proc. Eng.*, vol. 15, no. 1, pp. 3240–3244, 2011.

[31] H. Tang and J.-Z. Lin, "Inversion of visible optical extinction data for spheroid particle size distribution based on PCA," *Optik Int. J. Light Elect. Optic.*, vol. 125, no. 19, pp. 5494–5507, 2014.

[32] Q. Guo, W. Wu, D. L. Massart, C. Boucon, and S. de Jong, "Feature selection in principal component analysis of analytical data," *Chemometr. Intell. Lab. Syst.*, vol. 61, nos. 1–2, pp. 123–132, 2002.

[33] J. V. Manjón, P. Coupé, and A. Buades, "MRI noise estimation and denoising using non-local PCA," *Med. Image Anal.*, vol. 22, no. 1, pp. 35–47, 2015.

[34] C. Y. Yang and T. Y. Wu, "Diagnostics of gear deterioration using EEMD approach and PCA process," *Measurement*, vol. 61, pp. 75–87, Feb. 2015.

[35] (1989). *Ionosphere Database*. [Online]. Available: http://archive.ics.uci.edu//ml/machine-learning-databases/ionosphere/

[36] (1990). *Zoo Database*. [Online]. Available: http://archive.ics.uci.edu//ml/machine-learning-databases/zoo/

[37] (1997). *Contraceptive Method Choice Database*. [Online]. Available: http://archive.ics.uci.edu//ml/machine-learning-databases/cmc/

[38] N. R. Pal and J. C. Bezdek, "On cluster validity for the fuzzy c-means model," *IEEE Trans. Fuzzy Syst.*, vol. 3, no. 3, pp. 370–379, Aug. 1995.

[39] X. B. Gao, J. H. Pei, and W. X. Xie, "A study of weighting exponent m in a fuzzy c-means algorithm," *Acta Electron. Sinica*, vol. 28, no. 4, pp. 80–83, 2000.

[40] I. T. Jollie, *Principal Component Analysis*, 2nd ed. New York, NY, USA: Springer-Verlag, 2002.

[41] S. Narasimhan and N. Bhatt, "Deconstructing principal component analysis using a data reconciliation perspective," *Comput. Chem. Eng.*, vol. 77, pp. 74–84, Jun. 2015.

[42] Y.-L. He, X. Wang, and Q.-X. Zhu, "Modeling of acetic acid content in purified terephthalic acid solvent column using principal component analysis based improved extreme learning machine," *Control Theory Appl.*, vol. 32, no. 1, pp. 80–85, 2014.

[43] Y. M. Han and Z. Q. Geng, "Energy efficiency hierarchy evaluation based on data envelopment analysis and its application in a petrochemical process," *Chem. Eng. Technol.*, vol. 37, no. 12, pp. 2085–2095, 2014.

[44] Y. M. Han, Z. Q. Geng, X. B. Gu, and Z. Wang, "Performance analysis of China ethylene plants by measuring Malmquist production efficiency based on an improved data envelopment analysis cross-model," *Ind. Eng. Chem. Res.*, vol. 54, no. 1, pp. 272–284, 2015.

[45] *Calculation Method for Energy Consumption in Petrochemical Engineering Design*, Standard SH/T3110-2001, 2002.

Zhiqiang Geng received the B.Sc. and M.Sc. degrees from Zhengzhou University, Zhengzhou, China, in 1997 and 2002, respectively, and the Ph.D. degree from the College of Information Science and Technology, Beijing University of Chemical Technology, Beijing, China, in 2005.

He is currently a Professor of the College of Information Science and Technology, Beijing University of Chemical Technology. His current research interests include neural networks, intelligent computing, data mining, knowledge management, and process modeling. He has produced over 80 research papers in the above areas.

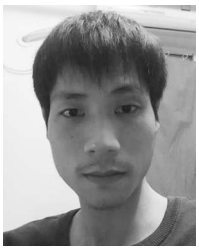

Jie Chen received the B.Sc. degree from the College of Information Science and Technology, Beijing University of Chemical Technology, Beijing, China, in 2014, where he is currently pursuing the M.Sc. degree.

His current research interests include artificial neural networks and intelligent computing.

Yongming Han received the B.Sc. and Ph.D. degrees from the Beijing University of Chemical Technology, Beijing, China, in 2009 and 2014, respectively.

He is currently a Lecturer of the College of Information Science and Technology, Beijing University of Chemical Technology. His current research interests include energy efficiency analysis, neural networks, intelligent computing, data mining, and energy saving.